Published in final edited form as:

Adv Funct Mater. 2017 November 24; 27(44): . doi:10.1002/adfm.201703726.

Ice-Templated Protein Nanoridges Induce Bone Tissue Formation

Prof. Mingying Yang,
Institute of Applied Bioresource Research, College of Animal Science, Zhejiang University, Yuhangtang Road 866, Hangzhou 310058, China

Dr. Yajun Shuai,
Institute of Applied Bioresource Research, College of Animal Science, Zhejiang University, Yuhangtang Road 866, Hangzhou 310058, China

Department of Chemistry & Biochemistry, Stephenson Life Sciences Research Center, University of Oklahoma, 101 Stephenson Parkway, Norman, OK 73019-5300, USA

Kegan S. Sunderland, and
Department of Chemistry & Biochemistry, Stephenson Life Sciences Research Center, University of Oklahoma, 101 Stephenson Parkway, Norman, OK 73019-5300, USA

Prof. Chuanbin Mao
Department of Chemistry & Biochemistry, Stephenson Life Sciences Research Center, University of Oklahoma, 101 Stephenson Parkway, Norman, OK 73019-5300, USA

School of Materials Science and Engineering, Zhejiang University, Hangzhou 310027, China

Abstract

Little is known about the role of biocompatible protein nanoridges in directing stem cell fate and tissue regeneration due to the difficulty in forming protein nanoridges. Here an ice-templating approach is proposed to produce semi-parallel pure silk protein nanoridges. The key to this approach is that water droplets formed in the protein films are frozen into ice crystals (removed later by sublimation), pushing the surrounding protein molecules to be assembled into nanoridges. Unlike the flat protein films, the unique protein nanoridges can induce the differentiation of human mesenchymal stem cells (MSCs) into osteoblasts without any additional inducers, as well as the formation of bone tissue in a subcutaneous rat model even when not seeded with MSCs. Moreover, the nanoridged films induce less inflammatory infiltration than the flat films in vivo. This work indicates that decorating biomaterials surfaces with protein nanoridges can enhance bone tissue formation in bone repair.

Correspondence to: Mingying Yang; Chuanbin Mao.

Supporting Information

Supporting Information is available from the Wiley Online Library or from the author.

Conflict of Interest

The authors declare no conflict of interest.

Keywords

bone; ice-templating; nanostructures; protein; stem cells

1. Introduction

Nanostructures made of inorganic or polymeric materials have been shown to control the stem cell fate or promote tissue formation.[1] As a physical factor, nanoscale structures on the surface of substrates may participate in directing the differentiation of stem cells. It was found that some nanostructures such as titania nanotubes could induce osteogenic differentiation without adding osteogenic supplements.[2] It was also found that the parallel microgrooves of polydimethylsiloxane could significantly enhance the efficiency of generating induced pluripotent stem cells[3] or direct the differentiation of human mesenchymal stem cells (MSCs) toward myogenic lineage.[4] However, little is known about how the nanostructures, such as nanoridges, made of pure biocompatible proteins, direct the differentiation of stem cells without any additional chemical inducers in vitro as well as the tissue formation in vivo. In fact, to the best of our knowledge, so far, there has been no report on the fabrication of nanoridges made of pure protein.

Bombyx mori silk fibroin (SF) is a natural fibrous protein and widely used as a biomaterial in tissue engineering.[5] It has features desired as a molecular building block for producing bone implants or tissue engineering scaffolds such as biocompatibility, robust mechanical properties, biodegradability, and processability.[6] Hence, SF can serve as a good model protein to study the potential of protein nanoridges in directing osteogenic differentiation of stem cells and bone tissue formation. Moreover, to overcome the challenge of fabricating protein nanoridges, here for the first time we developed an icetemplating method for the fabrication of protein nanoridges on the surface of SF materials. Then, we studied the effect of such nanoridges on the osteogenic differentiation of human MSCs as well as on the in vivo bone tissue formation (Scheme 1; Figure S1, Supporting Information).

2. Results and Discussion

2.1. Formation and Morphology of Nanoridges

In our ice-templating approach, first a flat SF film produced by a traditional method[7] was treated with methanol to become hydrophobic.[8] After methanol treatment, the resultant SF film is termed flat film because its surface was nearly flat (Figure 1B). Then it was incubated in H_2O. Due to the hydrophobic nature of the film which had a contact angle of 123°, the water droplets in the water-treated film tended to be spherical (Figure S2, Supporting Information). After the SF film was pulled out of H_2O slowly, it was immediately frozen in a temperature-controlled mould at −80 °C, during which water droplets were converted into ice crystals. We hypothesize that the expansion of volume accompanied with the conversion of water droplets into ice crystals[9] made the surrounding SF aggregated into nanoridges (Figure S1, Supporting Information). Finally, a freeze-drying process was used to convert ice into vapor, resulting in the formation of a SF film (termed nanoridged film, Figure 1C,D) with a unique nanoridged surface. We quantitatively analyzed the nanoridged structures and

found that the mean length of the nanoridges was about 932.2 ± 175.9 nm and the mean spacing between the nanoridges was about 640.6 ± 198.7 nm. Meanwhile, the macroscopic nanoridged film appeared opaque with white color while the flat film was transparent (Figure 1A).

2.2. Morphology, Proliferation, and Differentiation of MSCs on Nanoridges

Both flat and nanoridged SF films were able to support MSCs adhesion. However, the cells on the nanoridged films tended to be elongated, whereas those on the flat films remained spread (Figure 2A–D). Moreover, the cells on the flat surface proliferated faster than those on the nanoridged surface (Figure 2E). It was found that the slower cell proliferation tended to more favor the cell differentiation.[1d,10] Next, we further investigated the osteoblastic differentiation of MSCs on the flat or nanoridged SF films in the regular α-minimum essential medium (α-MEM) media (i.e., in the absence of any chemical inducers). A real-time polymerase chain reaction (PCR) assay was adopted to quantify the relative gene level of the osteogenic specific markers[11] including collagen I (COL), osteocalcin (OCN), osteopontin (OPN), and runt-related transcription factor 2 (RUNX2) (Figure 2F). The OCN gene showed a significantly higher mRNA level on the nanoridged films than on the flat films ($p < 0.05$). The COL, OPN, and RUNX2 genes exhibited an even higher mRNA level on the nanoridged films than on the flat films ($p < 0.01$). These data showed nanoridged SF films could trigger the osteoblastic differentiation without adding chemical inducers used in other studies[12] to the regular culture media, whereas the flat films could not.

This finding was further confirmed by the analysis of protein markers (OPN and OCN, the osteogenesis marker in the early and late stages of the osteogenic differentiation of MSCs, respectively)[11a] by immunofluorescence staining of MSCs on the flat and nanoridged SF films in the osteogenic differentiation medium or osteogenic induction-free medium for 14 d (Figures 3 and 4). It is likely that the nanoridged SF films induced osteogenic differentiation by promoting the elongation of the stem cells (Figure 2). We previously found that the cell elongation induced by the matrix would further induce the osteogenic differentiation.[11c,13]

Our results show that the protein nanoridges significantly accelerated the osteoblastic differentiation of MSCs without osteogenic inducing supplements. This is the first experimental data demonstrating that SF materials could induce the osteogenic differentiation of MSCs solely by controlling their surface nanotopography. Thus we proceeded to carry out in vivo evaluation of ectopic bone formation in a subcutaneous rat model, since this animal model is usually used to evaluate the bone inducing capability of a soft 2D material.

2.3. Risks of Nanoridges in Causing Immune Response

If a biomaterial can induce inflammatory responses in vivo, then it would affect how well the body heals itself during the earlier period after the biomaterial implantation. Consequently, in our in vivo study, we first investigated the risk of protein nanoridges in causing immune responses. After the flat and nanoridged SF films were implanted in the subcutaneous rat model for 4 weeks, new fibrous tissues were formed and almost no invading host cells were observed around all SF films based on the hematoxylin and eosin

(H&E) staining (Figure 5). The flat and nanoridged SF films did not show a significant difference in the thickness, suggesting the degradation rate of different SF films was almost the same. Multinucleated giant cells and fibrous cells surrounding biomaterial implants are one of the components of the inflammatory cells, and their participation may be linked to mast cell activation within a short time.[14] Our H&E staining (Figure 5) showed that the fibrous tissue and extracellular matrix were more dispersed around the nanoridged SF films than around the flat films, suggesting that the nanoridged SF films exerted less inflammatory cell infiltration and granulation tissue formation than the flat SF films after 4 weeks. Therefore, the animal test showed that less inflammatory infiltration was found in the nanoridged SF films than the flat SF films after implantation.

2.4. In Vivo Bone Formation Induced by Nanoridges

To find out whether protein nanoridges can induce bone formation, we implanted these SF films (with or without MSCs seeded) into subcutaneous dorsum sites of Sprague Dawley (SD) rats. Micro-computed tomography (micro-CT) data (Figure 6) showed no calcified tissue was formed on the flat films after one month of implantation. However, calcified tissues were observed on nanoridged films without MSCs implanted (Figure 6), implying that the implants with nanoridged topography were able to induce the formation of calcified tissue in ectopic sites of the subcutaneous model. When MSCs were seeded on the SF films, the flat films slightly induced some calcified tissue but the nanoridged films induced the formation of more calcified tissue. Furthermore, immunohistochemistry analysis (Figure 7) showed evidence of osteogenesis at the sites with the nanoridged films implanted but not at the sites with the flat films implanted after 4 weeks of implantation. Fibrous tissues around the nanoridged SF films with or without MSCs seeded were more organized and contained more collagen matrix deposition than those around the flat SF films with or without MSCs seeded, respectively. OPN and OCN staining showed the positive expression on the outer surface of SF films after 4 weeks even without seeding MSCs, suggesting that the amount of bone-like tissue clearly increased on all the nanoridged SF films compared to the flat SF films. However, the flat SF films showed a positive expression after 4 weeks only when seeded with MSCs. Therefore, micro-CT and histological evaluation showed the direct evidence for the formation of osteoid on the nanoridged films even without MSCs seeded.

To date, biomaterials induced calcified tissue formation in the ectopic model was found only when stem cells were seeded.[15] In our study, when MSCs were not seeded on the film implants, calcified tissue was observed on the nanoridged films 4 weeks after implantation (Figures 6 and 7). The reason for the material-induced bone formation in the subcutaneous model has not been made clear yet. One of the possible reasons is that the protein nanoridges had the biological functionality to recruit MSCs and minerals, which are available in the blood circulation system[16] surrounding the implants at the beginning of implantation. As a result, four weeks after implantation, the nanoridged SF films could further stimulate the differentiation of the recruited MSCs toward osteoblasts and promote the expression of bone matrix in vivo,[17] which was visible from the micro-CT and immunostaining results of the nanoridged films (Figures 6 and 7). Although other possible mechanisms of ectopic osteoinductivity of the nanoridged SF films should be further explored, we believe that the protein nanoridges are an important cue in stimulating bone formation.

3. Conclusion

In summary, we have presented a novel ice-templating processing approach to forming the protein nanoridges. The nanoridges reduced the cell proliferation and promoted cell elongation, which in turn could induce osteogenic differentiation. Moreover, the nanoridges had the capability of inducing the formation of calcified bone-like tissue with reduced inflammatory infiltration in a rat subcutaneous model even when no MSCs were seeded. Our work indicates that decorating biomaterials with protein nanoridges may be a new approach to enhanced bone tissue regeneration.

4. Experimental Section

Nanostructured Formation of SF Films

Cocoons were spun from *B. mori* silkworms. The pupa inside cocoons was removed by cutting a cocoon into small pieces. Then cocoon pieces were treated in Na_2CO_3 aqueous solution (0.25%) at 100 °C for 30 min to obtain SF fibers by removing the sericin coating on it (this processing is called degumming). The degummed SF fibers were dissolved in an aqueous $CaCl_2$ solution (with a mass concentration of 42%) at 100 °C for 5 min. The resultant mixture was subjected to dialysis against deionized water at 4 °C for a period of 3 d in order to remove $CaCl_2$ for collecting an aqueous SF solution. The regenerated fibroin was obtained and lyophilized. Then, the regenerated fibroin was dissolved in hexafluoro-2-propanol (HFIP) to prepare a SF solution with a concentration of 10 wt%.[18] A film was formed by casting SF on the Petri dish after the removal of HFIP by air-drying. Post-treatment was performed by soaking the film in methanol for 12 h to allow it to be insoluble in water. The procedure by this step is routine for preparing a SF film. The sole methanol treatment resulted in the formation of a SF film with a flat surface. To introduce nanoridges on the film surface, the hydrophobic film was soaked into deionized water for 12 h. The film was pulled out of the water, leaving discrete water droplets on the surface. The film was then immediately frozen in a temperature-controlled mould at −80 °C to form protein nanoridges, followed by lyophilization. This facile approach made the surface of the SF film nanostructured due to the nanoridge formation.

Cell Adhesion and Morphology on SF Films

The human MSCs used in this study were purchased from Lonza group Ltd. They were cultured in α-MEM medium (Gibco, US) supplemented with 10% fatal bovine serum (FBS) in a CO_2 incubator at 37 °C. The resultant medium is termed basal medium. Confluent cells were detached with 0.25% Trypsin-ethylene diamine tetraacetic acid (EDTA) (Gibco) and suspended in α-MEM supplemented with 10% FBS. Then MSCs with a density of 5×10^4 cells per well were seeded onto the flat and nanoridged SF film. Subsequently, an MTT assay was carried out to evaluate MSCs viability on SF films. For cell imaging, the cytoskeletons were stained by Alexa Fluor 488 (Alexa 488-conjugated phalloidin, Life Technologies) for 40 min at room temperature. The spreading pattern and morphology of MSCs were viewed using a confocal laser scanning microscope (CLSM, ZEISS LSM780, Germany).

Evaluation of Osteogenic Differentiation In Vitro

MSCs were cultured in basal medium and osteogenic induction medium, respectively. For osteogenic induction medium, the basal medium was supplemented with chemical inducers (100×10^{-9} M dexamethasone, 0.2×10^{-3} M ascorbic acid 2-phosphate, and 10×10^{-3} M β-glycerophosphate). The cells (2×10^4 cells per well) were seeded onto the flat and nanoridged SF film as well as tissue culture plate (TCP) as a control. After 2 weeks of culturing, the MSCs on the SF film substrates were used to evaluate the immunofluorescence staining of osteospecific markers. Briefly, the cells on SF films were fixed in 4% paraformaldehyde with 1 × phosphate buffered saline (PBS) for 30 min at room temperature. Then the fixed cells were permeated using 0.2% Triton X-100 for 10 min, followed by blocking with 5% bovine serum albumin (BSA)/1 × PBS solution for 30 min at room temperature. Subsequently, the cells were probed with the primary antibodies that recognize the osteospecific proteins, including OCN (1:500) and OPN (1:200), overnight at 4 °C, followed by washing and staining with secondary antibodies conjugated with rhodamine (1:1000) for 30 min at room temperature. After the samples were incubated with the secondary antibody, they were washed and then stained by FITC-labeled phalloidin (1:400 in PBS) and DAPI (4,6-diamidino-2-phenylindole) for probing the actin filaments and nuclei, respectively. The mRNA levels of osteogenesis-related genes (Col, OCN, OPN, RUNX2) in MSCs cultured on the flat films and the nanoridged SF films were analyzed using real-time PCR.

Subcutaneous Implantation Using Rat Subcutaneous Model

The human MSCs were seeded on the SF films by coculturing them in α-MEM medium for 5 d for promoting MSCs growth. Afterward, 20 SD rats (≈100 g) were used to evaluate histocompatibility and ectopic bone regeneration on the flat and nanoridged SF films with and without MSCs seeded using the rat subcutaneous model. Briefly, rats were randomized into 4 experimental groups, and each group included 8 animals for statistical analysis. For creating the animal model, the rats were anesthetized through inhaling a mixture of 4% isoflurane/oxygen using an anaesthesia machine. The rats were maintained during the surgical operation with 2% isoflurane delivered by a non-rebreathing system. SF films ≈10 mm × 10 mm were subcutaneously implanted onto the backs of SD rats. A subcutaneous injection of 2% lidocaine was administered immediately with the dosage of 1 mL kg^{-1} in the surgical area after the closure of the incision. Subsequently, in order to avoid infection, each rat was treated with penicillin intramuscularly for four consecutive days. The animals were sacrificed, and then films were extracted and fixed in 10% neutral formalin after 4 weeks of implantation.

Evaluation of Ectopic Bone Tissue Regeneration In Vivo

For micro-CT analysis, the film implants were subsequently scanned with a micro-CT (Scanco Medical, Switzerland) to determine the newly formed calcified tissue around the implants. After micro-CT analysis, the SF films were first processed, and embedded in paraffin by a Paraffin Embedder (Leica EG 1160). They were then sectioned into slices of a thickness of around 5 μm. The sections were further subjected to H&E staining to verify the histocompatibility and ectopic bone regeneration of the SF films. The immunohistochemical

staining for Col-I (Santa Cruz Biotechnology, sc-25974), OCN (Santa Cruz Biotechnology, sc-30044), and OPN (Santa Cruz Biotechnology, sc-21742) was performed to evaluate the formation of regenerated bone-like tissue[19] around the nanoridged SF film and the flat SF film. To stain the tissue, the sectioned slices were washed for three times in PBS and subsequently, endogenous peroxidase activity was blocked with a blocking reagent. They were then incubated for 20 min in normal serum and for 1.5 h with primary antibody at room temperature. After the sectioned slides were rinsed, they were treated with HRP-conjugated secondary antibody for 30 min. They were then washed with PBS. After then, appropriate chromagen with 3,3′-diaminobenzidine was added until desired staining intensity was achieved. The slides were then counterstained with hematoxylin and dehydrated through xylene.

Supplementary Material

Refer to Web version on PubMed Central for supplementary material.

Acknowledgments

The authors acknowledge the support of National Natural Science Foundation of China (51673168), Zhejiang Provincial Natural Science Foundation of China (LZ17C170002 and LZ16E030001), State of Sericulture Industry Technology System (CARS-18-ZJ0501), National High Technology Research and Development Program 863 (2013AA102507), Zhejiang Provincial Science and Technology Plans (2016C02054), and the National Key Research and Development Program of China (2016YFA0100900). Y.J.S., K.S.S., and C.B.M. would also like to thank the financial support from National Institutes of Health (CA200504, CA195607, and EB021339), Department of Defense office of the Congressionally Directed Medical Research Programs (W81XWH-15-1-0180), Oklahoma Center for Adult Stem Cell Research (434003), and Oklahoma Center for the Advancement of Science and Technology (HR14-160).

References

1. a) Dalby MJ, Gadegaard N, Oreffo RO. Nat Mater. 2014; 13:558. [PubMed: 24845995] b) Ahn EH, Kim Y, An SS, Afzal J, Lee S, Kwak M, Suh KY, Kim DH, Levchenko A. Biomaterials. 2014; 35:2401. [PubMed: 24388388] c) Kang K, Choi SE, Jang HS, Cho WK, Nam Y, Choi IS, Lee JS. Angew Chem, Int Ed. 2012; 51:2855.d) Dalby MJ, Gadegaard N, Tare R, Andar A, Riehle MO, Herzyk P, Wilkinson CD, Oreffo RO. Nat Mater. 2007; 6:997. [PubMed: 17891143] e) Tay CY, Koh CG, Tan NS, Leong DT, Tan LP. Nanomedicine. 2013; 8:623. [PubMed: 23560412] f) Yang M, Shuai Y, Zhou G, Mandal N, Zhu L, Mao C. ACS Appl Mater Interfaces. 2014; 6:13782. [PubMed: 25050697]
2. Oh S, Brammer KS, Li YJ, Teng D, Engler AJ, Chien S, Jin S. Proc Natl Acad Sci USA. 2009; 106:2130. [PubMed: 19179282]
3. Downing TL, Soto J, Morez C, Houssin T, Fritz A, Yuan F, Chu J, Patel S, Schaffer DV, Li S. Nat Mater. 2013; 12:1154. [PubMed: 24141451]
4. Yu T, Chua CK, Tay CY, Wen F, Yu H, Chan JK, Chong MS, Leong DT, Tan LP. Macromol Biosci. 2013; 13:799. [PubMed: 23606448]
5. a) Yang M, He W, Shuai Y, Min S, Zhu L. J Polym Sci, Part B: Polym Phys. 2013; 51:742.b) Rockwood DN, Preda RC, Yucel T, Wang X, Lovett ML, Kaplan DL. Nat Protoc. 2011; 6:1612. [PubMed: 21959241] c) Wang Q, Wang C, Zhang M, Jian M, Zhang Y. Nano Lett. 2016; 16:6695. [PubMed: 27623222] d) Perrone GS, Leisk GG, Lo TJ, Moreau JE, Haas DS, Papenburg BJ, Golden EB, Partlow BP, Fox SE, Ibrahim AM. Nat Commun. 2014; 5:3385. [PubMed: 24594992]
6. a) Altman GH, Diaz F, Jakuba C, Calabro T, Horan RL, Chen J, Lu H, Richmond J, Kaplan DL. Biomaterials. 2003; 24:401. [PubMed: 12423595] b) Vepari C, Kaplan DL. Prog Polym Sci. 2007; 32:991. [PubMed: 19543442] c) Kim HJ, Kim UJ, Kim HS, Li C, Wada M, Leisk GG, Kaplan DL. Bone. 2008; 42:1226. [PubMed: 18387349] d) Mandal BB, Grinberg A, Gil ES, Panilaitis B,

Kaplan DL. Proc Natl Acad Sci USA. 2012; 109:7699. [PubMed: 22552231] e) Hofmann S, Hilbe M, Fajardo RJ, Hagenmuller H, Nuss K, Arras M, Muller R, von Rechenberg B, Kaplan DL, Merkle HP, Meinel L. Eur J Pharm Biopharm. 2013; 85:119. [PubMed: 23958323]

7. a) Zhao C, Yao J, Masuda H, Kishore R, Asakura T. Biopolymers. 2003; 69:253. [PubMed: 12767126] b) Seib FP, Maitz MF, Hu X, Werner C, Kaplan DL. Biomaterials. 2012; 33:1017. [PubMed: 22079005]
8. a) Hu K, Gupta MK, Kulkarni DD, Tsukruk VV. Adv Mater. 2013; 25:2301. [PubMed: 23450461] b) Phillips DM, Drummy LF, Conrady DG, Fox DM, Naik RR, Stone MO, Trulove PC, De Long HC, Mantz RA. J Am Chem Soc. 2004; 126:14350. [PubMed: 15521743] c) Kundu B, Kurland NE, Bano S, Patra C, Engel FB, Yadavalli VK, Kundu SC. Prog Polym Sci. 2014; 39:251.
9. Pazhayannur P, Bischof J. J Biomech Eng. 1997; 119:269. [PubMed: 9285340]
10. Bacakova L, Filova E, Parizek M, Ruml T, Svorcik V. Biotechnol Adv. 2011; 29:739. [PubMed: 21821113]
11. a) Bassaw B, Roopnarinesingh S. West Indian Med J. 1990; 39:39. [PubMed: 2185595] b) Yang M, Shuai Y, Zhang C, Chen Y, Zhu L, Mao C, OuYang H. Biomacromolecules. 2014; 15:1185. [PubMed: 24666022] c) Wang J, Wang L, Li X, Mao C. Sci Rep. 2013; 3:1242. [PubMed: 23393624]
12. a) Langenbach F, Handschel J. Stem Cell Res Ther. 2013; 4:117. [PubMed: 24073831] b) Hayden RS, Quinn KP, Alonzo CA, Georgakoudi I, Kaplan DL. Biomaterials. 2014; 35:3794. [PubMed: 24484674]
13. Wang J, Wang L, Yang M, Zhu Y, Tomsia A, Mao C. Nano Lett. 2014; 14:6850. [PubMed: 25456151]
14. Thevenot PT, Nair AM, Shen J, Lotfi P, Ko CY, Tang L. Biomaterials. 2010; 31:3997. [PubMed: 20185171]
15. a) Akahane M, Nakamura A, Ohgushi H, Shigematsu H, Dohi Y, Takakura Y. J Tissue Eng Regener Med. 2008; 2:196.b) Vaquette C, Ivanovski S, Hamlet SM, Hutmacher DW. Biomaterials. 2013; 34:5538. [PubMed: 23623428] c) Lu J, He YS, Cheng C, Wang Y, Qiu L, Li D, Zou D. Adv Funct Mater. 2013; 23:3494.d) Ye X, Yin X, Yang D, Tan J, Liu G. Tissue Eng, Part C. 2012; 18:545.e) Tasso R, Gaetani M, Molino E, Cattaneo A, Monticone M, Bachi A, Cancedda R. Biomaterials. 2012; 33:2086. [PubMed: 22169138]
16. a) Chen Y, Xiang LX, Shao JZ, Pan RL, Wang YX, Dong XJ, Zhang GR. J Cell Mol Med. 2010; 14:1494. [PubMed: 19780871] b) Song G, Habibovic P, Bao C, Hu J, Van Blitterswijk CA, Yuan H, Chen W, Xu HH. Biomaterials. 2013; 34:2167. [PubMed: 23298780]
17. Tay CY, Muthu MS, Chia SL, Nguyen KT, Feng SS, Leong DT. Adv Funct Mater. 2016; 26:4046.
18. Rockwood DN, Preda RC, Yücel T, Wang X, Lovett ML, Kaplan DL. Nat Protoc. 2011; 6:1612. [PubMed: 21959241]
19. a) Hakki SS, Bozkurt SB, Hakki EE, Belli S. J Endodont. 2009; 35:513.b) Wang ZS, Feng ZH, Wu GF, Bai SZ, Dong Y, Chen FM, Zhao YM. Sci Rep. 2016; 6:28126. [PubMed: 27324079]

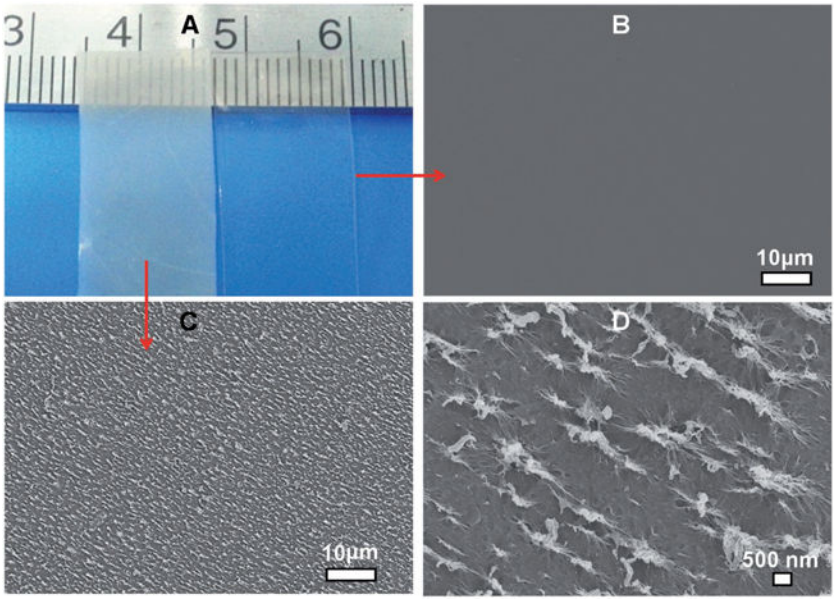

Figure 1.

Morphologies of flat and nanoridged SF films. The transparent and opaque films in (A) are the ones without and with nanoridge formation, respectively. The transparent film has a flat surface (B), whereas the surface of the opaque film is rough due to the presence of nanoridges surrounding nanopores (C). The higher magnification image of the rough surface shown in (C) indicated that nanoridges were indeed formed (D).

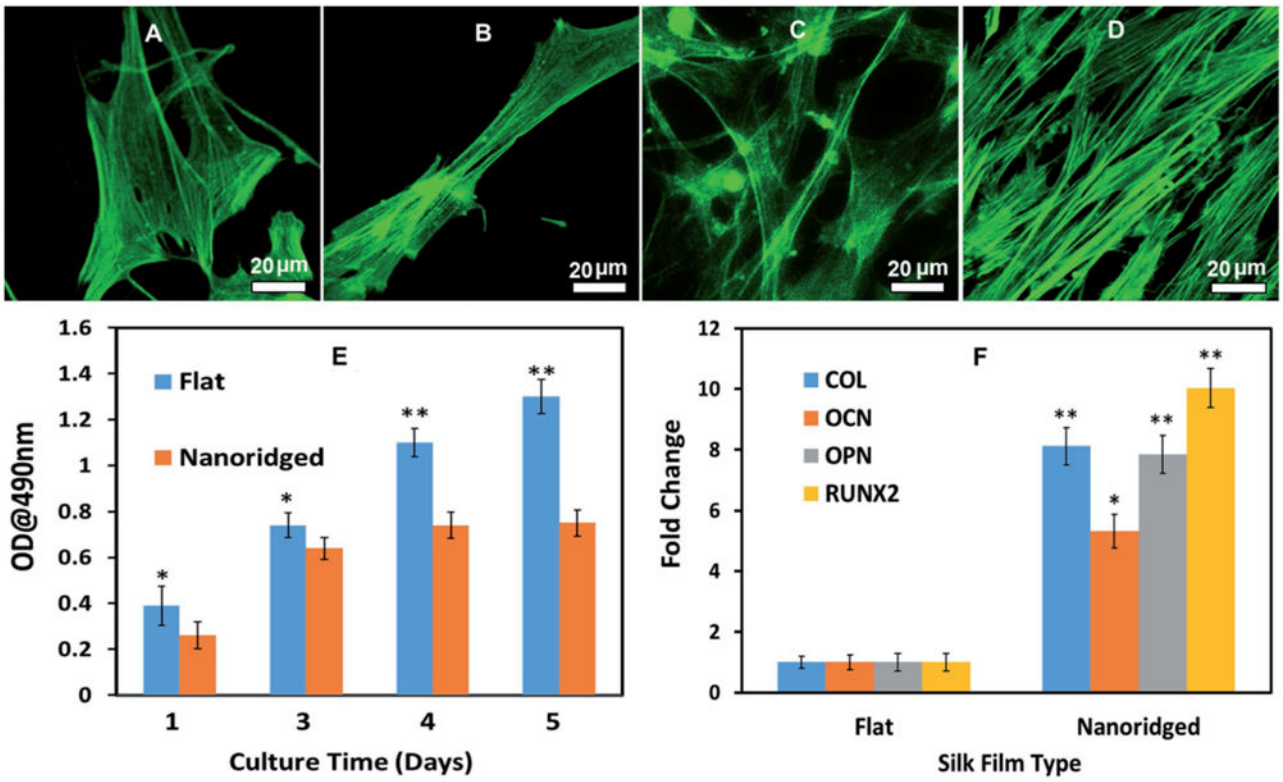

Figure 2.

Cell morphology (A–D), proliferation (E), and differentiation (F) on the flat and nanoridged SF film in basal medium. After the cells were cultured for 1 d (A, B) and 3 d (C, D), cell adhesion on the flat (A, C) and nanoridged SF film (B, D) showed that MSCs tended to be elongated on the nanoridged fibroin films. F-actin was stained by fluorescein isothiocyanate (FITC)-labeled phalloidin. 3-(4,5-Dimethylthiazol-2-yl)-2,5-diphenyltetrazolium bromide (MTT) assay (E) indicated that the flat surface enhanced a higher cell proliferation rate significantly, whereas real-time PCR (F) showed that the nanoridged films induced the osteogenic differentiation in the absence of additional inducers. All data represented the mean ± standard deviation (*$p < 0.05$, **$p < 0.01$).

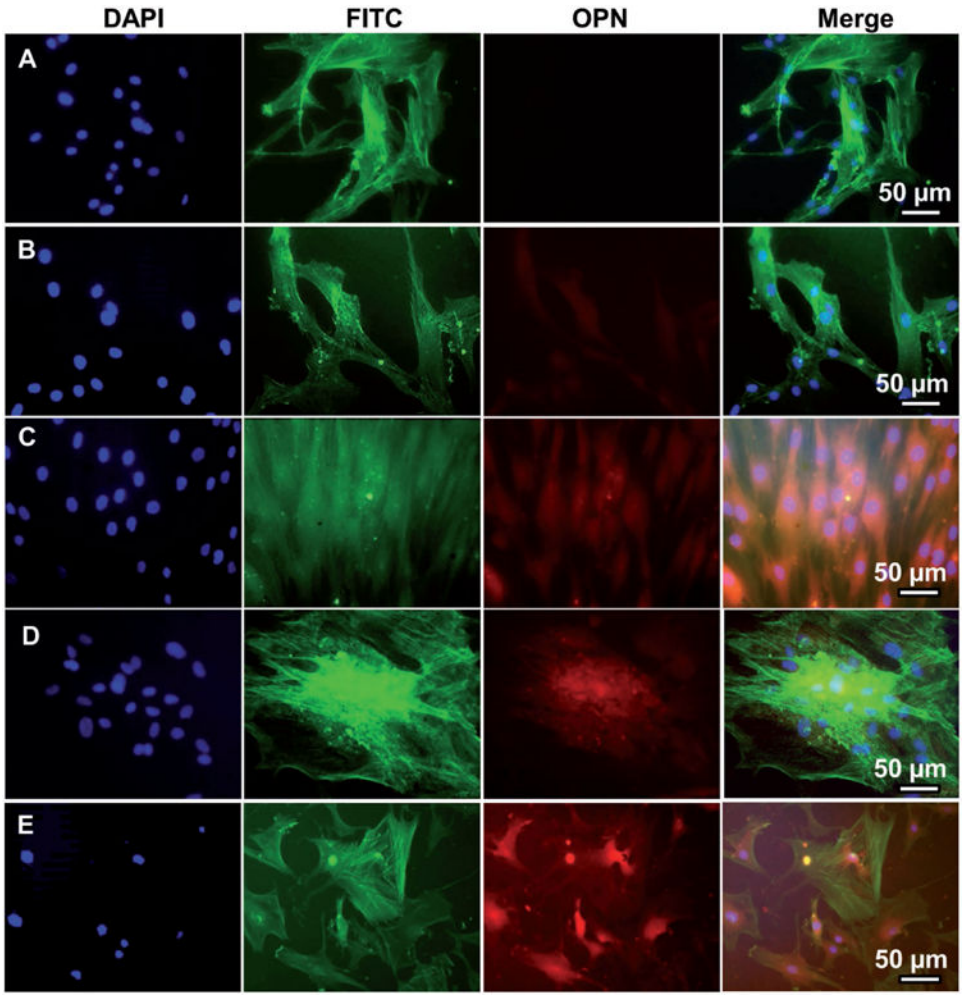

Figure 3.

Representative immunofluorescence images of OPN expression in human MSCs seeded on A) tissue culture plate (TCP) (A), flat (B, D), and nanoridged (C, E) SF films cultured in osteogenic induction-free medium (B, C) and osteogenic induction medium (D, E) on Day 14. The cells cultured on the nanoridged SF films (C) with osteogenic induction-free medium expressed more OPN than those cultured on TCP (A) and flat SF films (B) in the osteogenic induction-free medium. The cells cultured on both the flat (D) and nanoridged (E) films expressed OPN in the osteogenic induction medium. OPN was stained by rhodamine-labeled antibody (red) and cell nuclei were stained by 4′, 6-diamidino-2-phenylindole (DAPI) (blue) and F-actin was stained by FITC-labeled phalloidin (green).

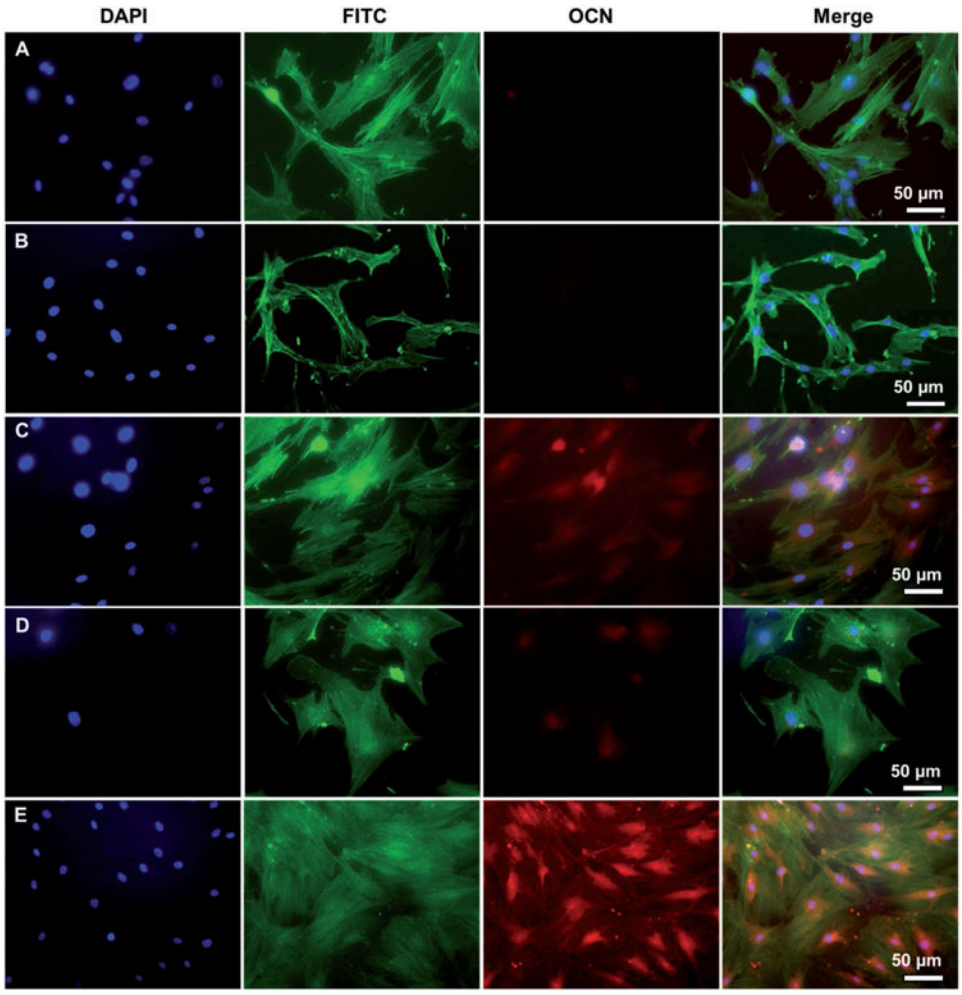

Figure 4.

Representative immunofluorescence images of OCN expression in human MSCs seeded on TCP (A), flat (B, D) and nanoridged (C, E) SF films cultured in osteogenic induction-free medium (B, C) and osteogenic induction medium (D, E) on Day 14. The cells cultured on the nanoridged SF films (C) with osteogenic induction-free medium expressed OCN, only slightly less than those cultured on the nanoridged SF films (E) with osteogenic induction medium. Moreover, cells cultured on TCP (A) and flat SF film (B) with osteogenic induction-free medium did not express OCN. Blue: DAPI nuclear staining; green: FITC actin staining; red: rhodamine-labeled antibody (red).

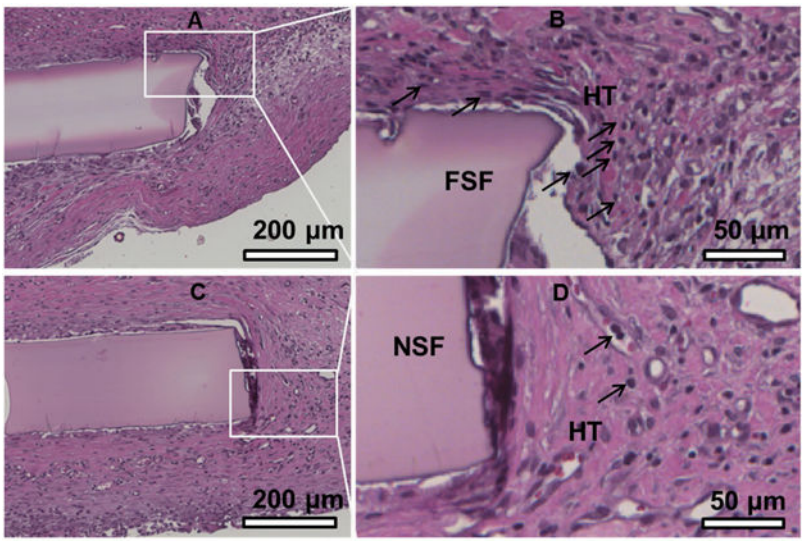

Figure 5.

Histological analysis of the flat SF film (A, B) and the nanoridged SF film (C, D) in subcutaneously implanted rat model after 4 weeks. The flat SF film shows strong and dense connective tissue staining (B), while the nanoridged SF film shows light and loose connective tissue staining (D). Furthermore, the H&E staining shows the formation of well-ordered collagen proteins and a small number of neutrophils around nanoridged SF film, while many neutrophils were observed around the flat SF film, suggesting less inflammatory cells and inflammatory responses in the nanoridged SF films than the flat SF films after 4 weeks of implantation. However, the overall inflammatory response to the nanoridged SF film and flat SF film were found to be mild. Black arrows indicate neutrophils. FSF: flat SF film; NSF: nanoridged SF film; HT: host tissues.

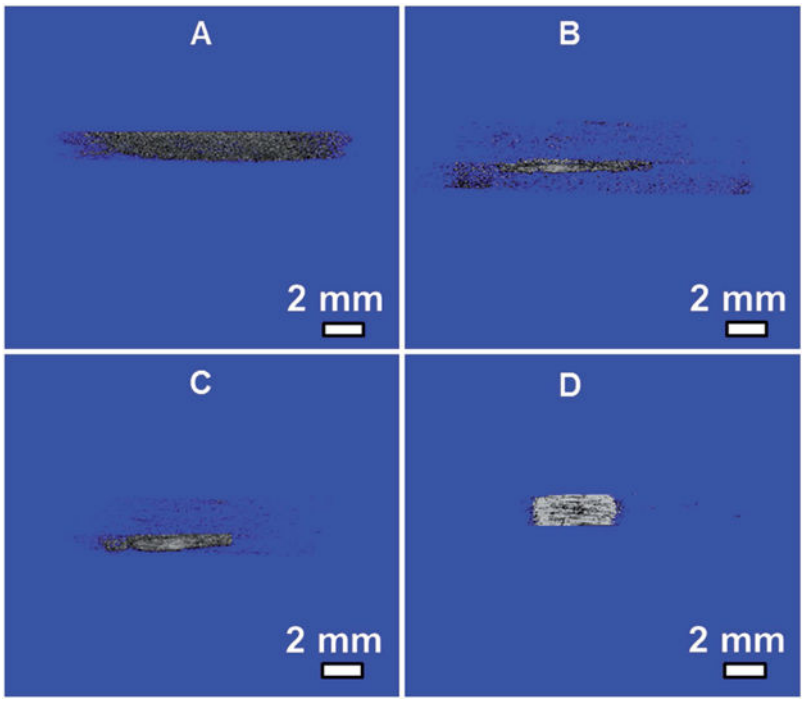

Figure 6.

Micro-CT imaging of heterotopic ossification of flat (A, B) and nanoridged SF films (C, D) in vivo after 4 weeks of implantation. Panels (A, C) without MSCs seeded on SF films before implantation. Panels (B, D) with MSCs seeded on SF films before implantation. Micro-CT images showed that calcified areas were discovered in the nanoridged SF film both without (C) and with (D) MSCs seeded and more calcified tissue was found in MSC-seeded nanoridged SF films (D) than in nonseeded nanoridged SF films (C).

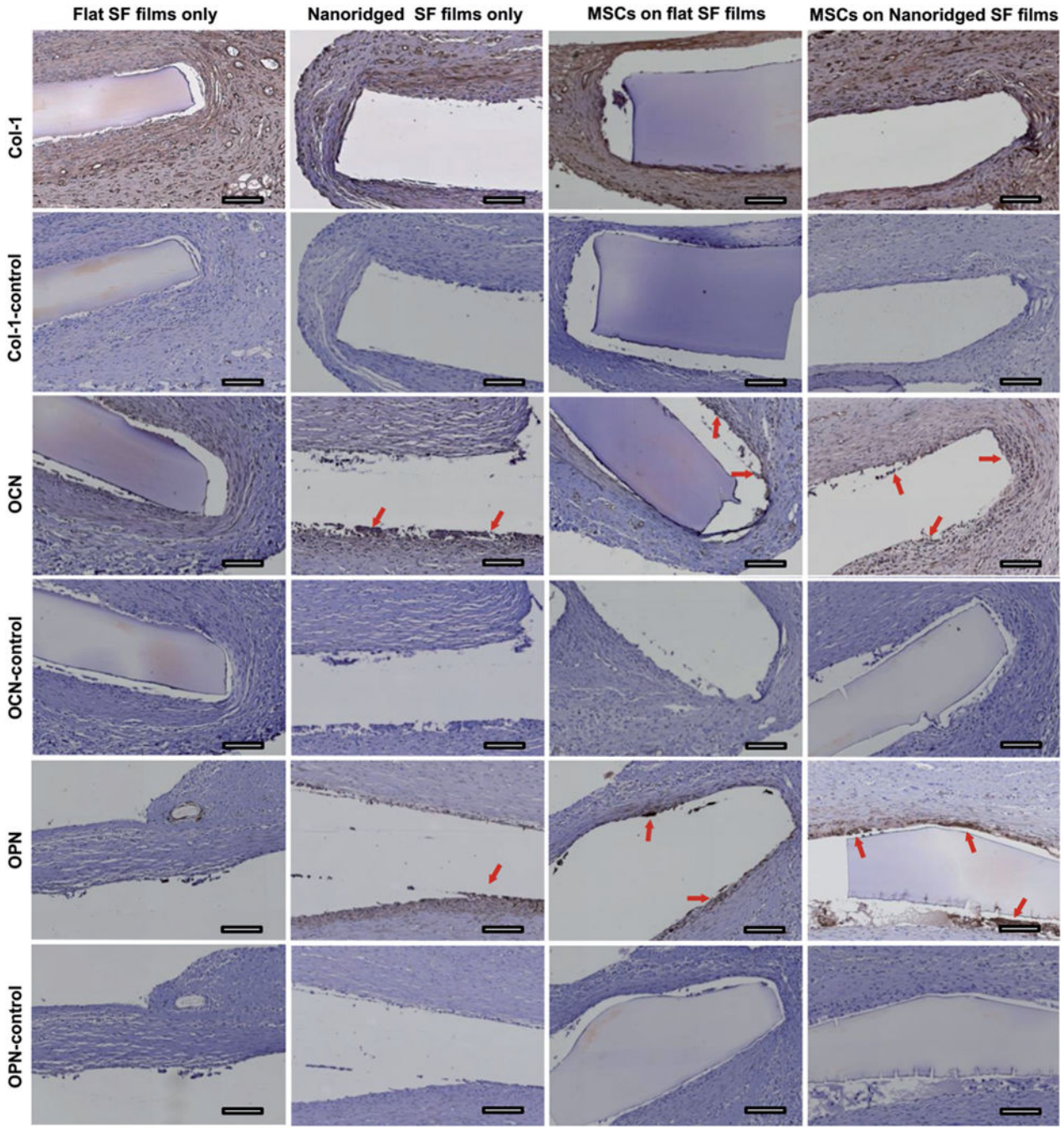

Figure 7.

Typical immunohistochemical staining for Col-I, OPN, and OCN within subcutaneously implanted flat SF films and nanoridged SF films with or without MSCs seeded after 4 weeks of implantation. Col-I control, OCN-control, and OPN-control groups were the histochemical staining slides only stained with hematoxylin. Col-I, OCN, and OPN groups were the immunohistochemical staining slides (from the same sectioned slices of Col-I control, OCN-control, and OPN-control, respectively) that were stained with a corresponding primary antibody, horseradish peroxidase (HRP)-conjugated secondary

antibody, and hematoxylin. The red arrows indicate the positively expressed bone matrix protein for each image. Immunohistochemical staining of SF film implants shows both MSCs seeded SF films and nanoridged SF films can induce the formation of new bone matrix proteins around the implanted SF films. Scale bar: 100 μm.

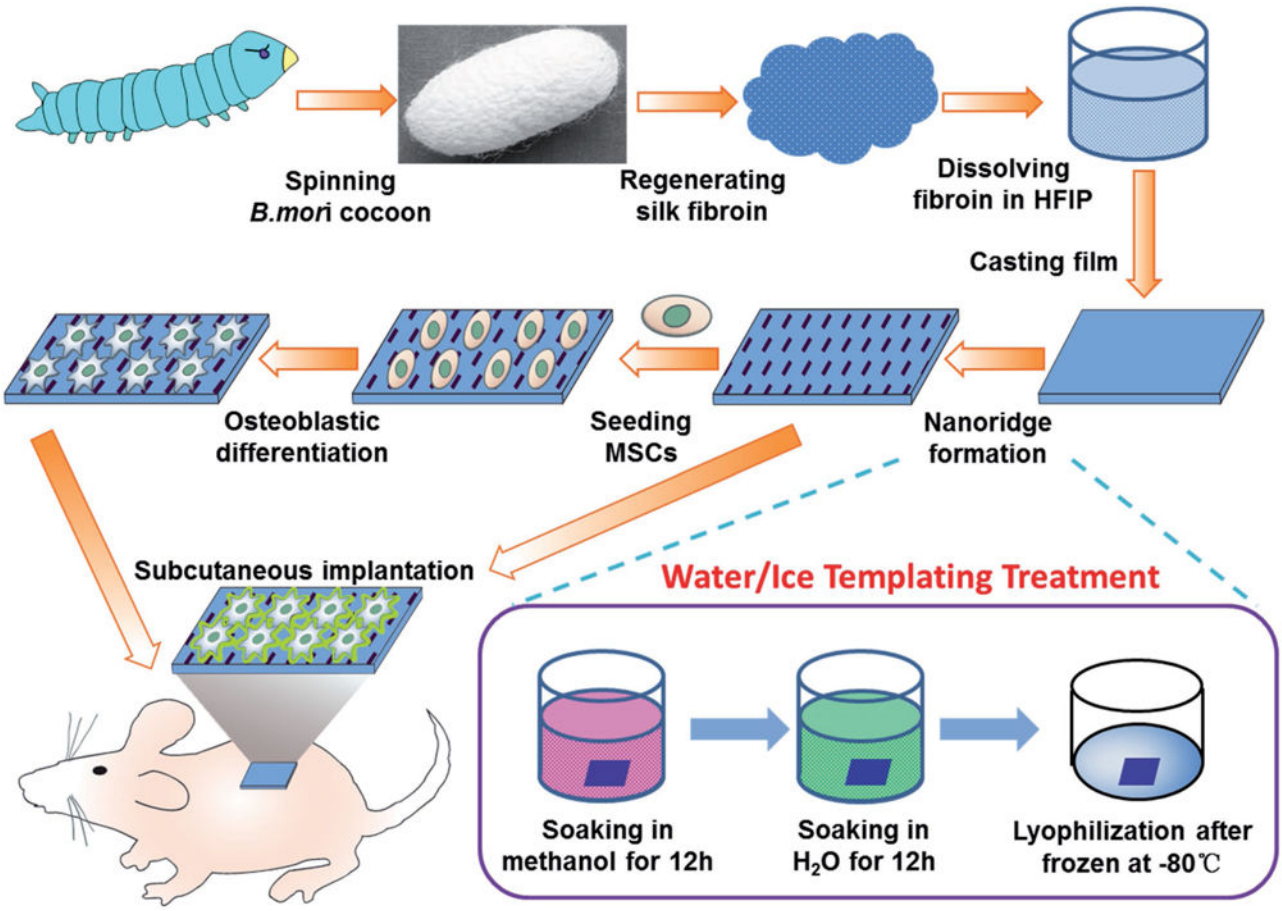

Scheme 1.

Schematic illustration of nanoridge formation on SF films by ice-templating to induce the osteogenic differentiation without additional osteogenic inducers and form ectopic bone in a rat subcutaneous model. SF was regenerated from cocoons and dissolved in hexafluoro-2-propanol (HFIP) for casting a film. The film was soaked in methanol to become hydrophobic and then in H_2O, followed by freezing and lyophilization to form nanoridges (Figure S1, Supporting Information). Nanoridges induce the osteogenic differentiation of MSCs cultured on the film without any additional chemical inducers. The nanoridged SF film can induce the formation of an osteoid matrix in a rat subcutaneous model with or without MSCs seeded.